Measurement of the $\eta \to 3\pi^0$ Dalitz Plot Distribution with the WASA Detector at COSY

The WASA-at-COSY Collaboration

C. Adolph[a], M. Angelstein[b,c], M. Bashkanov[d], U. Bechstedt[b,c], S. Belostotski[e], M. Berłowski[f], H. Bhatt[g], J. Bisplinghoff[h], A. Bondar[i], B. Borasoy[h], M. Büscher[b,c], H. Calén[j], K. Chandwani[g], H. Clement[d], E. Czerwiński[b,c,k], R. Czyżykiewicz[k], G. D'Orsaneo[b,c], D. Duniec[j,1], C. Ekström[l], R. Engels[b,c], W. Erven[m,c], W. Eyrich[a], P. Fedorets[n], O. Felden[b,c], K. Fransson[j], D. Gil[k], F. Goldenbaum[b,c], K. Grigoryev[b,c,o], A. Heczko[k], C. Hanhart[b,c], V. Hejny[b,c], F. Hinterberger[h], M. Hodana[b,c,k], B. Höistad[j], A. Izotov[e], M. Jacewicz[j,2], M. Janusz[b,c,k], B.R. Jany[b,c,k], L. Jarczyk[k], T. Johansson[j], B. Kamys[k], G. Kemmerling[m,c], I. Keshelashvili[b,c,3], O. Khakimova[d], A. Khoukaz[p], K. Kilian[b,c], N. Kimura[q], S. Kistryn[k], J. Klaja[b,c,k], P. Klaja[b,c,k], H. Kleines[m,c], B. Klos[r], A. Kowalczyk[b,c,k], F. Kren[d], W. Krzemień[b,c,k], P. Kulessa[s], S. Kullander[j], A. Kupść[j], A. Kuzmin[i], V. Kyryanchuk[b,c,4], J. Majewski[b,c,k], H. Machner[b,c,t], A. Magiera[k], R. Maier[b,c], P. Marciniewski[j], W. Migdał[k], U.–G. Meißner[b,c,h,u], M. Mikirtychiants[b,c,o], O. Miklukho[e], N. Milke[p,5], M. Mittag[b,c], P. Moskal[b,c,k], B.K. Nandi[g], A. Nawrot[f], R. Nißler[h], M.A. Odoyo[b,c], W. Oelert[b,c], H. Ohm[b,c], N. Paul[b,c], C. Pauly[b,c], Y. Petukhov[v], N. Piskunov[v], P. Pluciński[j], P. Podkopał[b,c,k], A. Povtoreyko[v], D. Prasuhn[b,c], A. Pricking[d,h], K. Pysz[s], J. Rachowski[w], T. Rausmann[p], C.F. Redmer[b,c], J. Ritman[b,c], A. Roy[g], R.J.M.Y. Ruber[j], Z. Rudy[k], R. Salmin[b,c,v], S. Schadmand[b,c], A. Schmidt[a], H. Schneider[b,c], W. Schroeder[a,6], W. Scobel[x], T. Sefzick[b,c], V. Serdyuk[b,c,y], N. Shah[g], M. Siemaszko[r], R. Siudak[b,c,h,s], T. Skorodko[d], T. Smoliński[b,c,k], J. Smyrski[k], V. Sopov[n], D. Spölgen[b,c], J. Stepaniak[f], G. Sterzenbach[b,c], H. Ströher[b,c], A. Szczurek[s], A. Teufel[a], T. Tolba[b,c], A. Trzciński[z], K. Ulbrich[h], R. Varma[g], P. Vlasov[b,c], W. Weglorz[b,c,r], A. Winnemöller[p], A. Wirzba[b,c], M. Wolke[b,c], A. Wrońska[k], P. Wüstner[m,c], H. Xu[aa], A. Yamamoto[q], H. Yamaoka[q], X. Yuan[b,c,aa], L. Yurev[b,c,y], J. Zabierowski[w], C. Zheng[b,c,aa], M.J. Zieliński[b,c,k], W. Zipper[r], J. Złomańczuk[j], K. Zwoll[m,c], I. Zychor[ab]

[a] *Physikalisches Institut, Universität Erlangen–Nürnberg, Erwin–Rommel-Str. 1, 91058 Erlangen, Germany*
[b] *Institut für Kernphysik, Forschungszentrum Jülich, 52425 Jülich, Germany*
[c] *Jülich Center for Hadron Physics, Forschungszentrum Jülich, 52425 Jülich, Germany*
[d] *Physikalisches Institut der Universität Tübingen, Auf der Morgenstelle 14, 72076 Tübingen, Germany*
[e] *The Few Body System Laboratory, High Energy Physics Division, St. Petersburg Nuclear Physics Institute, Orlova Rosha 2, 188300 Gatchina, Russia*
[f] *High Energy Physics Department, The Andrzej Soltan Institute for Nuclear Studies, ul. Hoza 69, 00-681, Warsaw, Poland*
[g] *Department of Physics, Indian Institute of Technology Bombay, Powai, Mumbai, 400076 Maharashtra, India*
[h] *Helmholtz–Institut für Strahlen– und Kernphysik, Rheinische Friedrich–Wilhelms–Universität Bonn, Nußallee 14–16, 53115 Bonn, Germany*
[i] *Budker Institute of Nuclear Physics, akademika Lavrentieva prospect 11, 630090 Novosibirsk, Russia*
[j] *Division of Nuclear and Particle Physics, Department of Physics and Astronomy, Uppsala University, Box 516, 75120 Uppsala, Sweden*
[k] *Institute of Physics, Jagiellonian University, ul. Reymonta 4, 30-059 Kraków, Poland*
[l] *The Svedberg Laboratory, Uppsala University, Box 533, 75121 Uppsala, Sweden*
[m] *Zentralinstitut für Elektronik, Forschungszentrum Jülich, 52425 Jülich, Germany*
[n] *Institute for Theoretical and Experimental Physics, State Scientific Center of the Russian Federation, Bolshaya Cheremushkinskaya 25, 117218 Moscow, Russia*
[o] *Cryogenic and Superconductive Techniques Department, High Energy Physics Division, St. Petersburg Nuclear Physics Institute, Orlova Rosha 2, 188300 Gatchina, Russia*
[p] *Institut für Kernphysik, Westfälische Wilhelms-Universität Münster, Wilhelm–Klemm–Str. 9, 48149 Münster, Germany*
[q] *High Energy Accelerator Research Organisation KEK, 1–1 Oho, Tsukuba, Ibaraki 305-0801 Japan*
[r] *August Chełkowski Institute of Physics, University of Silesia, Uniwersytecka 4, 40-007, Katowice, Poland*
[s] *The Henryk Niewodniczański Institute of Nuclear Physics, Polish Academy of Sciences, 152 Radzikowskiego St, 31-342 Kraków, Poland*
[t] *Fachbereich Physik, Universität Duisburg–Essen, Lotharstr. 1, 47048 Duisburg, Germany*
[u] *Bethe Center for Theoretical Physics, Rheinische Friedrich–Wilhelms–Universität Bonn, 53115 Bonn, Germany*
[v] *Veksler and Baldin Laboratory of High Energiy Physics, Joint Institute for Nuclear Physics, 141980 Dubna, Russia*
[w] *Department of Cosmic Ray Physics, The Andrzej Soltan Institute for Nuclear Studies, ul. Uniwersytecka 5, 90-950 Lodz, Poland*
[x] *Institut für Experimentalphysik der Universität Hamburg, Luruper Chaussee 149, 22761 Hamburg, Germany*
[y] *Dzhelepov Laboratory of Nuclear Problems, Joint Institute for Nuclear Physics, 141980 Dubna, Russia*
[z] *Department of Nuclear Reactions, The Andrzej Soltan Institute for Nuclear Studies, ul. Hoza 69, 00-681, Warsaw, Poland*
[aa] *Institute of Modern Physics, Chinese Academy of Sciences, 509 Nanchang Rd., 730000 Lanzhou, China*
[ab] *Department of Physics Applications, The Andrzej Soltan Institute for Nuclear Studies, 05-400 Otwock–Świerk, Poland*

Abstract

In the first production run of the WASA experiment at COSY, the eta decay into three neutral pions was measured in proton–proton interactions at a proton beam kinetic energy of 1.4 GeV. The Dalitz plot of the three pions was studied using 1.2×10^5 fully reconstructed events, and the quadratic slope parameter α was determined to be $-0.027 \pm 0.008(\text{stat}) \pm 0.005(\text{syst})$. The result is consistent with previous measurements and further corroborates the importance of pion–pion final state interactions.

Key words: η, $\eta \to 3\pi^0$, Dalitz plot
PACS: 13.25.-k, 12.75.Lb

1. Introduction

The η meson plays a special role in understanding low–energy Quantum Chromo Dynamics (QCD). Chiral symmetry, its realization in hadron physics at low energies and the role of explicit chiral symmetry breaking due to the masses of the light quarks (u, d, s) can be investigated using η decays.

The η meson decays into three pions ($\eta \to \pi^0\pi^0\pi^0$ and $\eta \to \pi^+\pi^-\pi^0$) are among the major decay modes (the branching ratios are 32.6% and 22.7%, respectively [1]) despite the fact that isospin is not conserved in these processes. It appears that these decays are driven by an isospin breaking term in the QCD Lagrangian which is proportional to the quark mass difference $m_d - m_u$ [2]. Any contribution from electromagnetic processes is suppressed [3, 4, 5]. The decay is closely related to pion–pion scattering, an elementary low–energy QCD process. The lowest order contribution to the decay mechanism is given by Current Algebra (CA) [6, 7]. The predicted partial decay width is more than four times lower than the measured value. On the other hand, the distributions of the decay products are described within a few percent accuracy.

The decay amplitude of η into three pions can be described using the following two Dalitz variables:

$$x \equiv \frac{1}{\sqrt{3}} \frac{T_1 - T_2}{\langle T \rangle}; \;\; y \equiv \frac{T_3}{\langle T \rangle} - 1. \tag{1}$$

Here T_i are the kinetic energies of the pions in the rest frame of the η meson, $3\langle T \rangle \equiv T_1 + T_2 + T_3 = m_\eta - 3m_\pi$ where m_π is the pion mass and the π^0, π^+ mass difference is neglected. The boundaries of the Dalitz plot are shown in Fig. 1.

The decay amplitude predicted by CA is a linear function of y for the $\eta \to \pi^+\pi^-\pi^0$ decay what implies that the $\eta \to \pi^0\pi^0\pi^0$ decay amplitude ($\bar{\mathcal{A}}$) is constant. Experimentally, a small deviation from a uniform Dalitz Plot density distribution is observed. The lowest term in the expansion about the center of the Dalitz plot is given by:

$$|\bar{\mathcal{A}}(z, \phi)|^2 = c(1 + 2\alpha z) \tag{2}$$

where z and ϕ variables are related to x and y via:

$$x = \sqrt{z}\cos\phi; \;\; y = \sqrt{z}\sin\phi. \tag{3}$$

c is a constant factor and α is the quadratic slope parameter.

The slope α was measured to be negative and small, which leads to a decrease of the Dalitz plot density at the border by a few percent. The explanation of this effect poses a challenge for Chiral Perturbation Theory (ChPT), the effective field theory of QCD in the low–energy region. The leading order calculations in ChPT coincide with CA whereas the next–to–leading order (NLO) calculations [8] significantly improve the agreement for the partial decay width but predict a small positive value for α. The large uncertainty of the recently carried out next–to–next–to–leading order (NNLO) calculations [9] does not allow to decide the sign of the slope. The origin of the non–uniform density distribution in the $3\pi^0$ Dalitz plot are in part pion–pion interactions in the final state. In contrast to the perturbative calculations, as soon as the rescattering effects are considered to infinite orders via unitarization of the decay amplitude using dispersion relations [10, 11] or iteration of the Bethe-Salpeter equation [12] the sign of α turns out to be in accordance with experiment. The calculations indeed predict negative values for α in agreement with the experimental results which are summarized in Table 1 together with the different theoretical predictions.

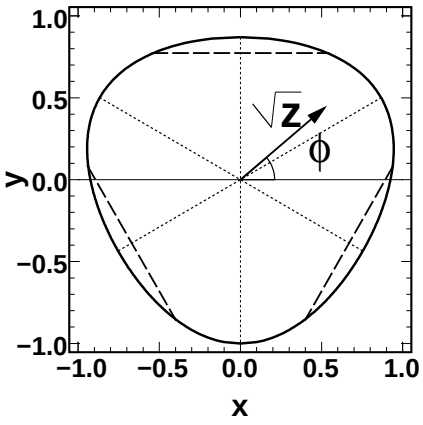

Figure 1: Symmetrized Dalitz plot for the $\eta \to \pi^0\pi^0\pi^0$ decay. Dashed lines represent threshold for $\pi^0\pi^0 \to \pi^-\pi^+$ rescattering.

Furthermore, $\eta \to 3\pi$ decays are considered to be a source of precise constraints for the light quark mass ratios [13]. In a recent approach the constraints are derived entirely from the experimental partial decay width and from the data on $\eta \to \pi^0\pi^0\pi^0$ Dalitz plot slope [14].

The first precise experimental determination of the α parameter was carried out by Crystal Ball at AGS [15] in 2001, using a pion beam impinging on a liquid hydrogen target. In 2005, KLOE released their first result of a high statistics measurement of α (using $e^+e^- \to \Phi \to \eta\gamma$) [16] which differed from the Crystal Ball result by three standard deviations. The CELSIUS/WASA [17] experiment has confirmed the negative sign of the slope parameter α. However, the achieved accuracy did not allow to resolve the discrepancy between the Crystal Ball and the early KLOE results. Very recently, the KLOE data were reanalyzed and a new α value was presented [18] that is consistent with Crystal Ball. However, the final results are not published yet. The Crystal Ball collaboration has recently collected

*Corresponding author

Email addresses: p.vlasov@fz-juelich.de (P. Vlasov)

[1]deceased

[2]present address: Laboratori Nazionali di Frascati, Via E. Fermi 40, 00044 Frascati, Italy

[3]present address: Departement für Physik, Universität Basel, Klingelbergstr. 82, 4056 Basel, Switzerland

[4]present address:Institute for Nuclear Research, Prospect Nauki 47, 03680 Kyiv, Ukraine

[5]present address: Technische Universität Dortmund, Experimentelle Physik 5B, Otto-Hahn-Straße 4, 44227 Dortmund, Germany

[6]present address: Unternehmensentwicklung und Außenbeziehungen, Forschungszentrum Jülich, 52425 Jülich, Germany

additional statistics at the MAMI facility that are currently being analyzed [19].

The phase space of the $\eta \to 3\pi^0$ decay covers the threshold for the $\pi^0\pi^0 \to \pi^+\pi^-$ rescattering process as a consequence of the fact that the neutral pion mass is slightly lower than the charged pion mass. The boundaries correspond to the $\pi^0\pi^0$ invariant mass being equal to $2m_{\pi^\pm}$. In 2004 a cusp like structure in the $\pi^0\pi^0$ invariant mass for the $K^+ \to \pi^0\pi^0\pi^+$ decay was observed by the NA48/2 collaboration [22]. The effect was predicted already in 1997 by Meißner et al. [23] and the interpretation of the NA48/2 results was given by Cabibbo [24]. The process provides a precise determination of a combination of the $I = 0$ and $I = 2$ pion–pion s-wave scattering lengths, a_0 and a_2. A similar effect was observed in the $K_L \to 3\pi^0$ decay [25] and it should be present also in the $\eta \to 3\pi^0$ and $\eta' \to \pi^0\pi^0\eta$ decays. There are important consequences of this phenomenon for the analysis of the $\eta \to 3\pi^0$ decay [26, 27, 28, 17, 29]. The amplitude is no longer a function only of the z variable but has to explicitly depend on the Mandelstam variables. The description of the amplitude as a polynomial function will fail in the cusp region. For example the dependence of the ϕ averaged amplitude squared ($|\bar{\mathcal{A}}|^2$):

$$|\bar{\mathcal{A}}|^2 \equiv \frac{1}{2\pi}\int_0^{2\pi} |\bar{\mathcal{A}}(z,\phi)|^2 d\phi \qquad (4)$$

on the z variable cannot be linear for $0.6 < z < 0.9$. However the most sensitive variables to search for the cusp effect are the invariant masses of the pion pairs (or kinetic energies of the pions). They correspond to the projections onto the dotted lines in Fig. 1.

The results presented in this paper are based on a measurement using proton–proton interactions with the WASA detection system recently installed at the Cooler Synchrotron COSY at the Forschungszentrum Jülich GmbH.

2. The experiment

The WASA detection system [30] was transported to COSY (COoler SYnchrotron) in the Summer 2005 [31]. The COSY facility at Jülich offers polarized and phase space cooled proton and deuteron beams with momenta up to 3.7 GeV/c [32, 33]. The available beam momentum range allows the production of π, K, η, ω, and $\eta\prime$ mesons well above the production thresholds in proton-proton and proton-deuteron interactions. Most of the final states in pN, pd, and dd reactions can be detected due to the nearly 4π acceptance of the WASA detector for charged and neutral particles.

The WASA detector [30] was designed and optimized for studies of production and decays of light mesons in hadronic interactions. It consists of three main components:
the Forward Detector - used for tagging and triggering on meson production, the Central Detector - used for measuring neutral and charged meson decay products, and the unique pellet target system. The target beam consists of 30 μm diameter pellets of hydrogen or deuterium, providing a high target density in the order of 10^{15} $atoms/cm^2$.

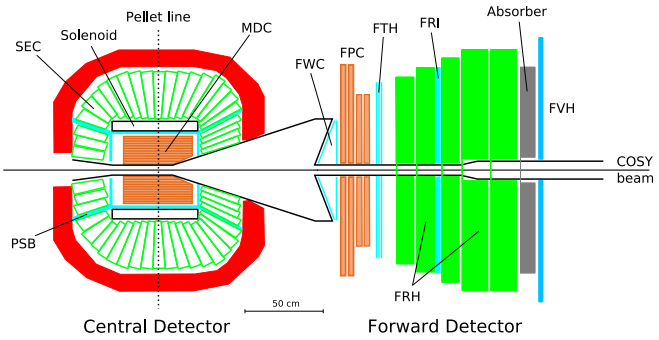

Figure 2: Schematic side view of the WASA detector setup at COSY.

The Central Detector surrounds the interaction region and is designed for detection and identification of photons, electrons, and charged pions. It consists of an inner drift chamber (MDC), a superconducting solenoid providing the magnetic field for momentum measurements, a barrel of thin plastic scintillators for particle identification and triggering, and an electromagnetic calorimeter. The amount of structural material is kept to a minimum to reduce disturbance of the particles. The beryllium beam pipe wall is 1.2 mm thick and the material of the superconducting solenoid corresponds to 0.18 radiation lengths.

The calorimeter (SEC) is used for detection and reconstruction of particles in the polar angle range from 20° to 169°, which is about 96% of the geometrical acceptance. The calorimeter consists of 1012 sodium doped CsI crystals. The trapezoidally shaped crystals with lengths from 20 to 30 cm correspond to ~16 radiation lengths. The energy resolution of the calorimeter is $\sigma(E)/E \approx 5\%/\sqrt{E[\mathrm{GeV}]}$ [30].

The forward detector is designed for detection of particles emitted in the polar angles from 3° to 18°. It allows for identification and reconstruction of protons from the $pp \to pp\eta$ reaction close to threshold. The precise track coordinates are given by four sets of straw proportional chambers (FPC). Kinetic energies are reconstructed using the ΔE information in the layers of plastic scintillators of different thickness. In addition, the signals are used for triggering. The kinetic energy of the protons can be reconstructed with a resolution of $\sigma(T)/T \sim 1.5 - 3\%$ for kinetic energies below 400 MeV.

The detector setup is nearly the same as used in the previous CELSIUS/WASA experiment [17]. The main change is a completely new readout system with charge-to-digital converters based on a flash ADC [34, 35]. In addition, the fourth layer of the forward range hodoscope (FRH) was replaced by two new thicker layers (15 cm instead of 11 cm).

The η mesons have been produced in proton–proton interactions at a beam proton energy of 1.4 GeV (momentum 2.141 GeV/c). The beam energy corresponds to a center of mass excess energy of 56 MeV for the $pp \to pp\eta$ reaction and the cross section is 10 μb. The results presented here are based on about 2.4 pb^{-1} of data collected during the first WASA-at-COSY production run and correspond to 94 hours of data taking. At the trigger level, events with two tracks in the forward detector and at least two hit groups in the calorimeter with en-

Slope parameter $\alpha \pm$ stat $\pm$ syst	Comment	year	Reference
-0.022 ± 0.023	GAMS-2000	(1984)	[20]
$-0.052 \pm 0.017 \pm 0.010$	Crystal Barrel	(1998)	[21]
$-0.031 \pm 0.004 \pm 0.004$	Crystal Ball	(2001)	[15]
$-0.014 \pm 0.004 \pm 0.005$	KLOE, preliminary	(2005)	[16]
$-0.027 \pm 0.004\ ^{+0.004}_{-0.006}$	KLOE, reanalysis	(2007)	[18]
$-0.026 \pm 0.010 \pm 0.010$	CELSIUS/WASA	(2007)	[17]
$-0.027 \pm 0.008 \pm 0.005$	WASA-at-COSY	(2008)	this result
0	CA	(1967)	[7]
+0.015	ChPT NLO	(1984)	[8]
$-(0.007 \div 0.014)$	ChPT NLO+dispersive	(1995)	[4]
-0.007	UChPT	(2003)	[11]
-0.031 ± 0.003	UChPT fit	(2005)	[12]
$+0.013 \pm 0.032$	ChPT NNLO	(2007)	[9]

Table 1: Overview of experimental and theoretical results for the slope parameter α.

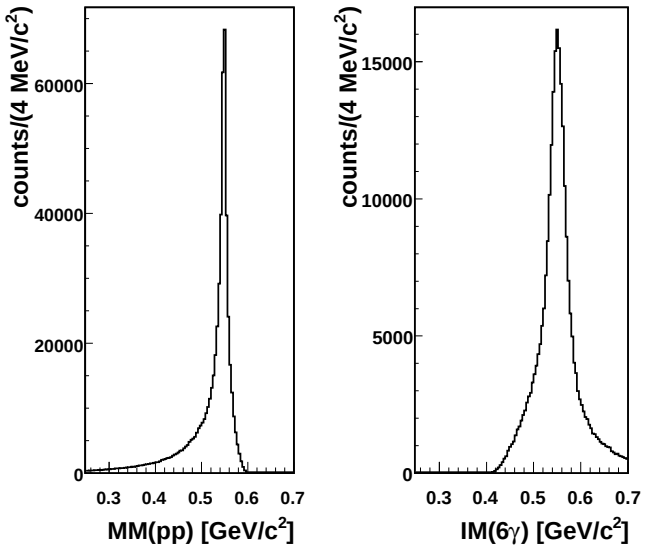

Figure 3: Missing mass of two protons, $MM(pp)$ (left) and invariant mass of six photons, $IM(2\gamma)$ (right) after selection of the $pp6\gamma$ final state.

ergy deposits of more than 50 MeV were accepted. In addition, a veto on signals in the plastic barrel (PSB) was required, aiming to select only neutral particles.

3. Data Analysis

In the offline analysis, the $pp6\gamma$ final state is selected by requiring six hit clusters with energy deposit at least 20 MeV in the calorimeter consistent with photons and two proton tracks in the forward detector. The conditions provide a clean data sample of about $8 \cdot 10^5$ events. In order to select π^0 candidates from the six reconstructed photons, all fifteen possible combinations of the three photon pairs were considered. For each combination, the quantity χ^2_j is calculated:

$$\chi^2_j \equiv \sum_i^3 \frac{(IM(j,i) - m_{\pi^0})^2}{\sigma^2}, \qquad j = 1, 2, 3, ...15 \tag{5}$$

where $IM(j,i)$ is the invariant mass of the i-th $\gamma\gamma$ pair for the j-th combination, $\sigma = 14$ MeV/c^2 is the resolution of the $\gamma\gamma$ invariant mass. The combination with minimum value of χ^2_j is selected. Only events with $\chi^2_j < 15$ and a missing mass of two protons between 0.535 GeV/c^2 and 0.565 GeV/c^2 are kept. Fig. 3 shows the missing mass of two protons (left panel) and the invariant mass of six photons (right panel) after applying the cut on the missing mass and after fitting the individual pions.

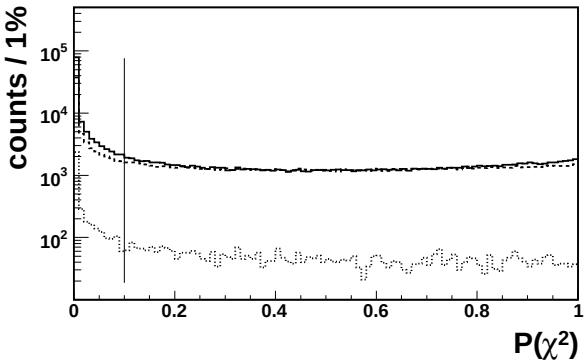

Figure 4: The distribution of the kinematic fit probability with the $\eta \to 3\pi^0$ decay hypothesis ($P(\chi^2)$) for the experimental data (solid line), Monte Carlo simulation of the signal (dashed line), and background (dotted line). The vertical line represents the selection for the final Dalitz plot analysis.

In order to reconstruct the $3\pi^0$ Dalitz plot, a kinematic fit is applied. In ref. [17], the full final state including the two protons was considered in the fitting procedure. Here, only the $\eta \to 3\pi^0$ decay system is fitted, based on the reconstructed photon angles and momenta. This approach reduces systematic uncertainty due to proton reconstruction. Different reconstruction uncertainties (as a function of energy and angle) were obtained from a full GEANT Monte Carlo detector simulation, with resolution parameters matched to reproduce experimental distributions. The experimental distribution of the kinematic fit probability ($P(\chi^2)$) is compared in Fig. 4 to the Monte Carlo simulation. The simulation includes background from direct three pion production, $pp \to pp\pi^0\pi^0\pi^0$, the cross section was obtained by interpolation of the results from the CELSIUS/WASA experiment [36]. The relative amount of background is less than 4% in the final event sample after $P(\chi^2) > 0.1$ cut (vertical line in Fig. 4).

4. Extraction of the slope parameter

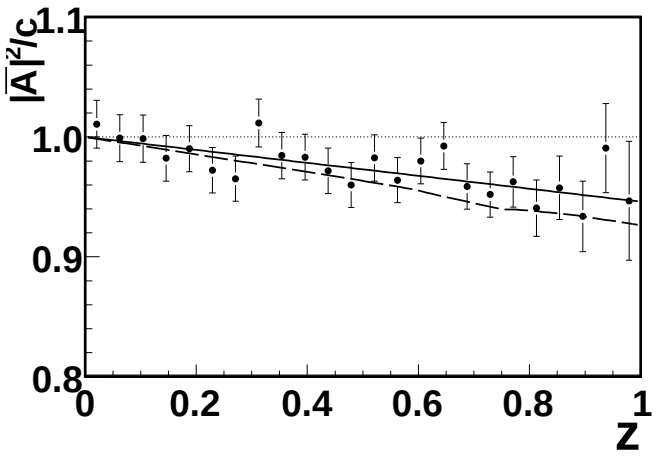

Figure 5: Extracted dependence of $|\bar{\mathcal{A}}|^2$ on the z variable. The solid line is a $c(1 + 2\alpha z)$ fit. The dashed line is a prediction of the cusp effect [37].

Based on the analysis procedure, the efficiency corrected radial density distribution $|\bar{\mathcal{A}}|^2$ is shown in Fig. 5. The efficiency correction is obtained by dividing the measured z distribution by the result of the Monte Carlo simulation, assuming $\alpha = 0$. A linear fit to the data points is applied to extract the slope parameter α, yielding a statistical uncertainty of $\sigma(\alpha) = 8 \cdot 10^{-3}$. The achieved resolution in z is $\sigma(z)$=0.055.

The systematic uncertainty of the result is estimated by varying one by one all parameters that are important in the analysis. Table 2 summarizes some of these studies. The dominant contribution comes from an uncertain fraction of the interactions with gas stemming from pellet evaporation or with pellets bouncing in the beam pipe. This causes a spread in the vertex position.

The combinatoric purity of the selected event sample depends on the cut on χ^2_j probability of the best combination and on the confidence level of the fit. A variation of these parameters has only a minor effect on the obtained slope result.

Another source of systematic errors is imposed by the remaining background. This effect is under control by changing the width of the proton–proton missing mass cut and, hence, varying the relative amount of background in the range from 4 % to 12 %. The observed effect contributes with 0.002 to the slope parameter uncertainty.

The kinematic fit performance relies on the precise understanding of the errors of reconstructed quantities. This effect was studied by replacing the polar angle dependent parametrization of reconstruction uncertainties with a much simpler polar angle independent description, again showing only a small effect on the result (see table 2).

Source of systematic uncertainty	RMS
Combinatoric background	0.001
Missing mass cut	0.002
Background $3\pi^0$ production	0.001
Vertex position	0.004
Confidence level cut	0.001
Error parametrization for the kinematical fit	0.002
Overall systematic uncertainty	0.005

Table 2: The main contributions to the systematic uncertainty as discussed in the text. The overall systematic uncertainty was calculated as the square root of the summed squares of all contributions.

Taking into account the systematic studies, the final result for the extracted slope parameter α is

$$\alpha = -0.027 \pm 0.008(stat) \pm 0.005(syst)$$

based on 120000 events. The result agrees within one standard deviation with the high statistics measurements of the slope parameter performed by the KLOE collaboration [18] and the Crystal Ball collaboration [15]. It is also consistent with the previous measurement performed by the CELSIUS/WASA collaboration [17]. The shape of the z distribution including the cusp that emerges from a virtual $\pi^+\pi^-$ intermediate state followed by a $\pi^+\pi^- \to \pi^0\pi^0$ transition, can be calculated from the $\eta \to \pi^+\pi - \pi^0$ amplitude and the $\pi - \pi$ scattering lengths. The cusp effect leads to a broad local minimum in the radial density of the Dalitz plot for $0.6 < z < 0.9$ due to the contribution of the regions where the invariant mass of the two pions less than $2m_{\pi^\pm}$ (see Fig. 1). The dashed line in Fig. 5 was obtained using a parameterization of the $\eta \to \pi^+\pi^-\pi^0$ decay amplitude from the KLOE collaboration [38] and a nonrelativistic effective field theory [29, 37]. It is seen that the statistical precision of the data is insufficient to investigate the cusp effect.

5. Outlook

One motivation for the presented study was the striking discrepancy between KLOE and Crystal Ball results for the $\eta \to$

$3\pi^0$ Dalitz plot slope parameter α. Now, after the recent reanalysis of the KLOE data, the three major experiments focusing on the measurement of η decays, KLOE at DAPHNE in Frascati, Crystal Ball now installed at MAMI in Mainz, and WASA-at-COSY in Jülich, obtain consistent results. The non–zero value of the slope parameter is clear indication for the importance of final state pion–pion interactions. The theoretical understanding of these processes has advanced significantly, also triggered by the firm experimental situation. The Dalitz plot slope parameter provides a very sensitive test of the ChPT predictions. The ChPT NLO and NNLO calculations that assume $m_{\pi^0} = m_{\pi^\pm}$ in the loops, indicate a positive sign of the slope parameter. The uncertainty is however large and the negative sign is not excluded [9].

Among the experiments studying η decays, WASA is presently the only experiment focusing on hadronic production of eta mesons in pp or pd scattering. The experiment combines the high production cross section especially in the pp reaction with the capability to run at high luminosities up to $10^{32} cm^{-2} s^{-1}$. This will allow to collect high statistics data samples of η mesons (10^7 decays and more) with WASA-at-COSY. High statistics data samples provide further increased accuracy and sensitivity in the study of small effects, like the cusp structure in $\eta \to 3\pi^0$. Recently WASA-at-COSY has collected a large data sample of $pd \to {}^3\mathrm{He}\eta$ events with low background and an unbiased trigger requirement, enabling studies *e.g.* of $\eta \to \pi^0\pi^0\pi^0$ and $\eta \to \pi^+\pi^-\pi^0$ decays simultaneously.

6. Acknowledgments

This work was in part supported by: the Forschungszentrum Jülich including the COSY-FFE program, the European Community under the FP6 program (Hadron Physics, RII3-CT-2004-506078), the German BMBF, the german-indian DAAD-DST exchange program, VIQCD (VH-VI-231) and the German Research Foundation (DFG).

We gratefully acknowledge the financial support given by the Knut and Alice Wallenberg Foundation, the Swedish Research Council, the Göran Gustafsson Foundation, the Polish Ministry of Science and Higher Education under grants PBS 7P-P6-2/07, 3240/H03/2006/31, 1202/DFG/2007/03,

We also want to thank the technical and administration staff at the Forschungszentrum Jülich and at the participating institutes.

This work is part of the PhD Thesis of P. Vlasov.

References

[1] **Particle Data Group** Collaboration, C. Amsler *et al.* *Phys. Lett.* **B667** (2008) 1.
[2] J. Bijnens and J. Gasser *Phys. Scripta* **T99** (2002) 34, arXiv:hep-ph/0202242.
[3] D. G. Sutherland *Nucl. Phys.* **B2** (1967) 433.
[4] R. Baur, J. Kambor, and D. Wyler *Nucl. Phys.* **B460** (1996) 127, arXiv:hep-ph/9510396.
[5] C. Ditsche, B. Kubis, and U.-G. Meißner 2008. in preparation.
[6] W. A. Bardeen, L. S. Brown, B. W. Lee, and H. T. Nieh *Phys. Rev. Lett.* **18** (1967) no. 25, 1170.
[7] H. Osborn and D. J. Wallace *Nucl. Phys.* **B20** (1970) 23.
[8] J. Gasser and H. Leutwyler *Nucl. Phys.* **B250** (1985) 539.
[9] J. Bijnens and K. Ghorbani *JHEP* **11** (2007) 030, arXiv:0709.0230 [hep-ph].
[10] J. Kambor, C. Wiesendanger, and D. Wyler *Nucl. Phys.* **B465** (1996) 215, arXiv:hep-ph/9509374.
[11] N. Beisert and B. Borasoy *Nucl. Phys.* **A716** (2003) 186, arXiv:hep-ph/0301058.
[12] B. Borasoy and R. Nißler *Eur. Phys. J.* **A26** (2005) 383, arXiv:hep-ph/0510384.
[13] H. Leutwyler *Phys. Lett.* **B378** (1996) 313, arXiv:hep-ph/9602366.
[14] A. Deandrea, A. Nehme, and P. Talavera *Phys. Rev.* **D78** (2008) 034032, arXiv:0803.2956 [hep-ph].
[15] **Crystal Ball** Collaboration, W. B. Tippens *et al.* *Phys. Rev. Lett.* **87** (2001) 192001.
[16] **KLOE** Collaboration, S. Giovannella *et al.* in *Proceedings of La Thuile 2005, Results and perspectives in particle physics*, p. 241. Rencontres de Moriond, 2005. arXiv:hep-ex/0505074.
[17] **CELSIUS/WASA** Collaboration, M. Bashkanov *et al.* *Phys. Rev.* **C76** (2007) 048201, arXiv:0708.2014 [nucl-ex].
[18] **KLOE** Collaboration, F. Ambrosino *et al.* in *Proceedings of LP07 conference*, pp. S8–356. Kyungpook National University Press, 2007. arXiv:0707.4137 [hep-ex].
[19] A. Starostin and S. Prakhov. In the Proceedings of 11th International Conference on Meson-Nucleon Physics and the Structure of the Nucleon (MENU 2007), Julich, Germany, 10-14 Sep 2007.
[20] **Serpukhov-Brussels-Annecy(LAPP)** Collaboration, D. Alde *et al.* *Z. Phys.* **C25** (1984) 225.
[21] **Crystal Barrel** Collaboration, A. Abele *et al.* *Phys. Lett.* **B417** (1998) 193.
[22] **NA48/2** Collaboration, J. R. Batley *et al. Phys. Lett.* **B633** (2006) 173, hep-ex/0511056.
[23] U.-G. Meißner, G. Müller, and S. Steininger *Phys. Lett.* **B406** (1997) 154, arXiv:hep-ph/9704377. Erratum-ibid.B407:454,1997.
[24] N. Cabibbo *Phys. Rev. Lett.* **93** (2004) 121801, hep-ph/0405001.
[25] **KTeV** Collaboration, E. Abouzaid *et al. Phys. Rev.* **D78** (2008) 032009, arXiv:0806.3535 [hep-ex].
[26] N. Cabibbo and G. Isidori *JHEP* **03** (2005) 021, arXiv:hep-ph/0502130.
[27] E. Gamiz, J. Prades, and I. Scimemi *Eur. Phys. J.* **C50** (2007) 405, arXiv:hep-ph/0602023.
[28] G. Colangelo, J. Gasser, B. Kubis, and A. Rusetsky *Phys. Lett.* **B638** (2006) 187, arXiv:hep-ph/0604084.
[29] M. Bissegger, A. Fuhrer, J. Gasser, B. Kubis, and A. Rusetsky *Phys. Lett.* **B659** (2008) 576, arXiv:0710.4456 [hep-ph].
[30] **CELSIUS/WASA** Collaboration, C. Bargholtz *et al.* *Nucl. Instrum. Meth.* **A594** (2008) 339, arXiv:0803.2657 [nucl-ex].
[31] **WASA-at-COSY** Collaboration, H. H. Adam *et al.* arXiv:nucl-ex/0411038.
[32] D. Prasuhn *et al. Nucl. Instrum. Meth.* **A362** (1995) 16.
[33] R. Maier *Nucl. Instrum. Meth.* **A390** (1997) 1.
[34] H. Kleines *et al. IEEE Trans. Nucl. Sci.* **53** (2006) 893.
[35] H. Kleines *et al. IEEE Trans. Nucl. Sci.* **55** (2008) 261.
[36] **CELSIUS/WASA** Collaboration, C. Pauly *et al.* *Phys. Lett.* **B649** (2007) 122, arXiv:nucl-ex/0602006.
[37] A. Rusetsky, A. Kupsc, and C.-O. Gullstrom 2008. in preparation.
[38] **KLOE** Collaboration, A. Antonelli *et al. JHEP* **05** (2008) 006, arXiv:0801.2642 [hep-ex].